Pertanika J. Sci. & Technol. 32 (1): 419 - 436 (2024)

PERTANIKA JOURNALS

SCIENCE & TECHNOLOGY

Journal homepage: http://www.pertanika.upm.edu.my/

Preparation of Activated Carbon from Sugarcane Bagasse Using Microwave-assisted $ZnCl_2$ Chemical Activation: Optimization and Characterization Study

Atiqa Rahmawati[1]*, Fadzkurisma Robbika[1] and Yuafni[2]

[1]*Department of Leather Processing Technology, Politeknik ATK Yogyakarta, Special District of Yogyakarta, Yogyakarta, Indonesia*

[2]*Department of Leather Product Technology, Politeknik ATK Yogyakarta, Special District of Yogyakarta, Yogyakarta, Indonesia*

ABSTRACT

Microwave-assisted activation is a green technology technique that can synthesize activated carbon from bagasse. In this study, microwave-assisted $ZnCl_2$ chemical activation was applied to convert bagasse to activated carbon (BAC). Activating activated carbon was optimized using surface response methodology (RSM). The Box-Behnken (BBD) design was used to assist in the optimum synthesis condition, with the loading of $ZnCl_2$ concentration (A: 10–50% w/v), heating time (B: 2–12 min), and microwave power (C: 150–800 W). The BAC was characterized using Brunauer-Emmett-Teller (BET), Scanning Electron Microscopy (SEM), Fourier Transform Infrared (FT-IR), and moisture content. The findings of the BAC optimization were at a $ZnCl_2$ concentration of 24.281 (% w/v), 12 min of heating time, and 800 W of microwave power. The characterization result shows that BAC_{op} has mesoporous carbon and a desirable surface area of 446.874 m^2/g, average pore size of 4.071 nm, pore volume of 0.054 cc/g, and total pore volume of 0.2531 cc/g. SEM analysis revealed that microwave-generated pore structures lead to the $ZnCl_2$ activation process. The pore structures of the raw material and activated carbon were different. The FT-IR analysis shows the existence of functional groups as well as changes in functional groups from raw material to activated carbon. The moisture content study findings are 5.51 to 9.21% in accordance with the Indonesian National Standard (SNI) 06-3730-1995. The isothermal adsorption-desorption process is classified as type IV adsorption with hysteresis loop H4, suggesting that the pore distribution in activated carbon is mesoporous with a tiny pore width and slit-shape pore materials.

Keywords: Activated carbon, box-behnken, microwave-assisted activation, optimization, sugarcane bagasse, $ZnCl_2$

ARTICLE INFO

Article history:
Received: 20 February 2023
Accepted: 20 July 2023
Published: 15 January 2024

DOI: https://doi.org/10.47836/pjst.32.1.22

E-mail addresses:
tiqa054@gmail.com (Atiqa Rahmawati)
Fadzkurisma.risma@gmail.com (Fadzkurisma Robbika)
yuafni@atk.ac.id (Yuafni)
*Corresponding author

ISSN: 0128-7680
e-ISSN: 2231-8526

© Universiti Putra Malaysia Press

INTRODUCTION

Biomass waste as a feedstock for renewable energy or the development of material innovation is a challenge in research (Daochalermwong et al., 2020). The significant increase in biomass waste is getting much attention due to environmentally friendly aspects and the availability of raw materials, which is also one aspect of sustainable development (Ummartyotin & Pechyen, 2016). Using biomass waste as raw material for material innovation or renewable energy has developed methods and is still being developed to meet industrial needs. One of the developments focuses on the use of biomass waste as an adsorption material known as an adsorbent (Ummartyotin & Pechyen, 2016). Activated carbon is an amorphic compound produced from materials with a high carbon level and is specially modified to produce a larger surface area (Arnelli et al., 2019). On an industrial scale, activated carbon is utilized as an adsorbent for purification and separation processes (Ozdemir et al., 2014). Hence, it is utilized in wastewater treatment, metal recovery, solvent recovery, food processing, and improving odor and flavor (Ao et al., 2018).

Several studies have produced activated carbon from various biomass wastes such as sugarcane bagasse (el Nemr et al., 2022; Foo et al., 2013; Jiang et al., 2021; Karri et al., 2020; Kaushik et al., 2017; Salihi et al., 2017), macadamia nut endocarp (Junior et al., 2014), pineapple leaf (Daochalermwong et al., 2020), rice husk (Arnelli et al., 2019), grape stalk (Ozdemir et al., 2014), cotton stalk (Deng et al., 2009), sludge waste (Bian et al., 2018), rubber fruit shell (Suhdi & Wang, 2021) and many more. Based on the study's findings, biomass waste can be converted into low-cost adsorbents (Buthiyappan et al., 2019). Activated carbon preparation from lignocellulose often uses physical or chemical activation (Abdulhameed et al., 2021). The physical activation process involves the carbonization of raw materials under inert conditions, followed by the activation of the resultant carbon at high temperatures (Mahmood et al., 2017). In contrast, chemical activation consists of a single step. It is conducted in the presence of dehydrating reagents such as KOH, K_2CO_4, NaOH, $ZnCl_2$, and H_3PO_3, which inhibit tar formation and enhance pyrolytic decomposition (Deng et al., 2009). In this study, we used a combination of chemical and physical activation to improve activated carbon characteristics. Lam et al. (2017) state that combining chemical and physical activation will produce activated carbon with highly accessible pores. $ZnCl_2$, as an activator in chemical activation, was used for its advantages in generating activated carbon with small pore volume, pore size, and higher surface area (Luo et al., 2019). Furthermore, microwaves can affect activated carbon's pore structure and surface area (Arnelli et al., 2019).

Sugarcane Bagasse is one of the biomass wastes that can be developed into activated carbon. Sugarcane bagasse comprises approximately 50% cellulose, 25% hemicellulose, and 25% lignin, each reacting vigorously with dyestuff and heavy metals (Buthiyappan et al., 2019). However, unmodified sugarcane bagasse has limited absorption efficiency, long

contact time, and low pH sensitivity. Sugarcane bagasse can be chemically and physically modified to generate low-cost activated carbon and efficiently remove heavy metals, dyestuffs, and phenols (Buthiyappan et al., 2019). The availability of sugarcane bagasse based on Indonesian Plantation Research Center (P3GI) data, from 62 sugar factories, 29,911 million tonnes of sugarcane can be milled per year, resulting in 2,991 million tonnes of bagasse will be produced (Hidayati et al., 2016). Meanwhile, up to 3,500 tonnes of sugarcane is used daily at the Madukismo Sugar Factory in Yogyakarta, and 1,400 tonnes of bagasse are generated daily. 50% of the bagasse produced by the milling process will be used as boiler feed, the others being stored as waste with no economic value. Bagasse can be used as a raw material for producing activated carbon for adsorption due to the high carbon concentration of the lignocellulose in bagasse (Hidayati et al., 2016).

Activated carbon is composed of functional groups bound to fused aromatic rings, which are predicted to have comparable chemical characteristics to aromatic hydrocarbons. Thermal, hydrothermal, or chemical treatment can alter and adjust surface functional groups in carbon matrices for specific applications (Ao et al., 2018). To optimize the activated carbon preparation from bagasse, we used Response Surface Methodology (RSM). RSM was chosen in some recent studies to optimize the preparation parameters and further analyze potential interaction between various parameters (Yuan et al., 2018). Box-Behnken Design (BBD) is one of the RSM commonly used in food processing, analytical chemistry, and AC production. BBD provides the following advantages: BBD assists in optimizing variables with the fewest number of experiments, contributes further analysis interaction between variables, can effectively estimate factors of the quadratic model, and avoids combination factors at an extreme range (Yuan et al., 2018).

This study converted bagasse from the Madukismo sugar factory in Yogyakarta, Indonesia into activated carbon. Chemical and physical activation were combined to prepare activated carbon. The activation was performed using microwave-assisted $ZnCl_2$ chemical activation. This study aims to optimize activated carbon (AC) production from sugarcane bagasse using $ZnCl_2$ as a precursor in chemical activation and microwave-assisted activation as physical activation. Optimization of activated carbon used RSM. The BBD design was approached in the optimum synthesis condition. The effect of microwave power, heating time, and $ZnCl_2$ concentration on activated carbon was investigated. In addition, BET surface area, iodine number, surface functional group analysis by Boehm titration, FT-IR analysis, and SEM-EDX were used to characterize the bagasse-activated carbon.

METHODOLOGY

Activated Carbon (AC) Preparation

Raw Material. Sugarcane Bagasse (SB) was obtained from Madukismo Sugar Factory, Yogyakarta, Indonesia. Sugarcane bagasse was washed with distilled water several times

to remove the dirt and dried in an oven at 110°C for 24 hrs. The material was subsequently pulverized and granulometrically into particles with sizes 177 µm. The proximate examination of the raw material was performed at Pusat Studi Pangan dan Gizi Gadjah Mada University, Indonesia to determine the concentration of hemicellulose, cellulose, and lignin.

Synthesis of Activated Carbon. Conventional pyrolysis and microwave-assisted $ZnCl_2$ chemical activation were utilized to prepare the activated carbon. Sugarcane bagasse was placed in a furnace and heated at a rate of 15°C/min from 30 to 500°C for one hour. The generated char is properly preserved in a plastic container for further activation. The activation process for activated carbon consists of two steps: chemical and physical. The first step is chemical activation. In 50 ml of $ZnCl_2$ solution, the carbon is submerged for 12 hrs at impregnation ratios of 10% w/v (low factor level), 30% w/v (midpoint), and 50% w/v (high factor level). The carbon was subsequently reactivated (second step) using a conventional microwave oven (Samsung ME731K 2.45 gHz) and subjected to different heating times (min) and microwave radiation (W). Table 1 shows the combination of variables for the optimization process. The optimization process of activated carbon was performed in duplicate for each combination variable. The resulting material was repeatedly rinsed with 0.1 M HCl and distilled water until the pH of the solution dropped to 7.0. The resulting AC was separated, dried at 110°C for 24 hrs, and stored for further analysis.

Table 1
Real variables and levels in BBD experimental design

Factors	Coded value		
	-1	0	+1
$ZnCl_2$ concentration, A (% w/v)	10	30	50
Heating time, B (min)	2	7	12
Microwave power, C (W)	150	450	800

Box-Behnken Experimental Design. Response surface methodology with Box Behnken Design (BBD) was used to examine the interaction between variables and response in the activated carbon activation (Junior et al., 2014). In this study, independent variables A, B, and C were altered (-1, 0, +1), with the iodine number of activated carbon (mg/g) as the dependent variable. Table 1 shows the variable combinations utilizing the BBD. The BBD experimental design employs 15 experiments with 12 factorial and 3 central points. Response prediction (Y) can be determined using a second-order polynomial regression model (Equation 1) (Junior et al., 2014; Yuan et al., 2018).

$$Y = b_0 + \sum_{i=1}^{k} b_i x_i + \sum_{i=1}^{k} b_{ii} x_i^2 + \sum_{i=1}^{k-1} \sum_{j=2}^{k} b_{ij} x_i x_j \qquad [1]$$

Where Y is the predicted response value, x_i and x_j are real or code variables, b_0 represents the constant term, b_i represents the linear effect term, b_{ii} represents the quadratic effect term, and b_{ij} represents the interaction effect term (Yuan et al., 2018). The experimental data regression model and statistical significance model were assessed using analysis of variance (ANOVA). Design Expert is utilized for design experiment development, model evaluation, and optimization.

Characterization of Activated Carbon

Moisture Meter MA 45 Sartorius obtained the water content of activated carbon. 1±0.2 gram activated carbon was placed in an aluminum container, then heated at 105°C until the constant weight reached. Moisture content was displayed when the process finished. The iodine number was determined using the sodium thiosulfate volumetric method (Siragi et al., 2021). The iodine number is a relative indicator of porosity in activated carbon and can be used to estimate the surface area of activated carbon. The pore size of activated carbon can be approximated by analyzing the iodine number >1.0 nm (Özhan et al., 2014). The surface area of activated carbon was determined by Brunauer-Emmet-Teller (BET). Pore structure and pore distribution were evaluated by nitrogen adsorption at 77 K using NOVA 2000 Quantrachrome. Scanning electron microscopy (SEM) was performed using Jeol JSM-6510 LA, surface morphology analysis for sugarcane bagasse, carbon, and activated carbon. The functional group of raw material, carbon, and activated carbon was analyzed and identified by Fourier transform infrared spectrometer (FTIR-Perken Elmer frontier) in the scanning range 4000–700 cm^{-1}.

RESULTS AND DISCUSSION

Carbonization of Sugarcane Bagasse

Table 2 shows the results of sugarcane bagasse's hemicellulose, cellulose, and lignin. Important factors in the carbonization process are carbonation temperature and biomass composition, such as lignin, hemicellulose, and cellulose (Pratama et al., 2018). Cellulose and hemicellulose are chemically similar, the main difference being the number of saccharide units. Meanwhile, lignin is a hydrophobic compound and can inhibit water penetration. The cellulose content in bagasse will be more easily decomposed due to the thermal breakdown of the sugar in the bagasse. In addition, the decomposition of cellulose will produce volatile components (Pratama et al., 2018). Thermal decomposition of hemicellulose occurs at a temperature of 200°C, followed by the decomposition of cellulose at a temperature range of 250–400°C (Ukanwa et al., 2019), while the minimum temperature of lignin is decomposed at 500°C (Hidayati et al., 2016). In this study, the carbonation was carried out at a temperature of 500°C so that the volatile components of the biomass would evaporate, and pore formation occurred in the carbon. In the process, the carbonation and

Table 2
Composition of sugarcane bagasse from Madukismo Sugar Factory, Yogyakarta, Indonesia

Sample	Content		
	Hemicelulose (%)	Celulose (%)	Lignin (%)
Sugarcane Bagasse	24.81	39.67	19.61
	24.18	40.99	18.93
Average	24.295	40.330	19.270

activation of volatile compounds evaporate from cellulose and hemicellulose. The more volatile compounds evaporate, the more pores are formed. It will result in a decrease in yield and an increase in adsorption power (Elsayed & Zalat, 2015). The yield from the carbonation process is 26%.

Response Surface Methodology and Statistical Analysis of Activated Carbon

Figures 1, 2, and 3 showed three-dimensional response surfaces for two factors. The effect of heating time on the iodine number is shown in Figures 1 and 2. Figures 1 and 2 show that the iodine number increases with heating time. Activated carbon in the sample has become dehydrated, contributing to the rise in iodine concentration (Baytar, Şahin, Saka, & Ağrak, 2018). The amount of energy transmitted to the precursor of activated carbon rises as the heating time of the microwave increases (Junior et al., 2014). In addition, prolonged microwave radiation promotes the formation of activated carbon, which has a large number of pores and active sites and improves its capability to adsorb chemicals. Furthermore, when the radiation time reaches a certain value, it can reduce the value of

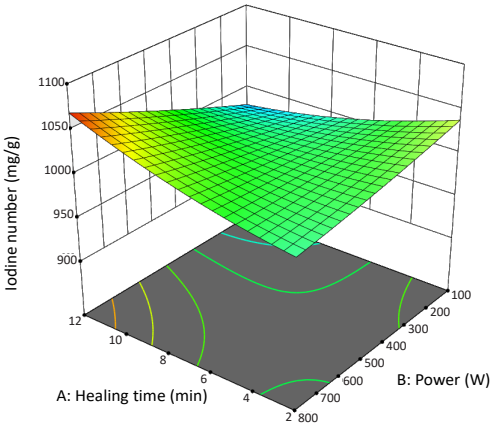

Figure 1. Three-dimensional response surface of iodine number for interaction between heating time and microwave power

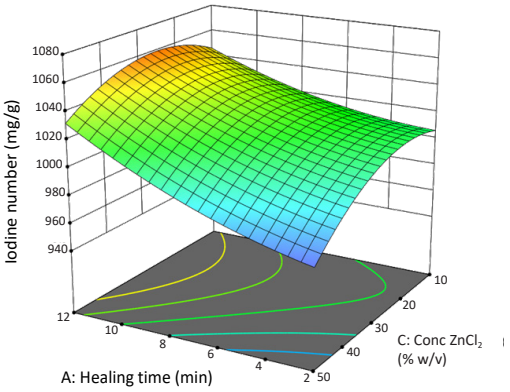

Figure 2. Three-dimensional response surface of iodine number for interaction between heating time and $ZnCl_2$ concentration

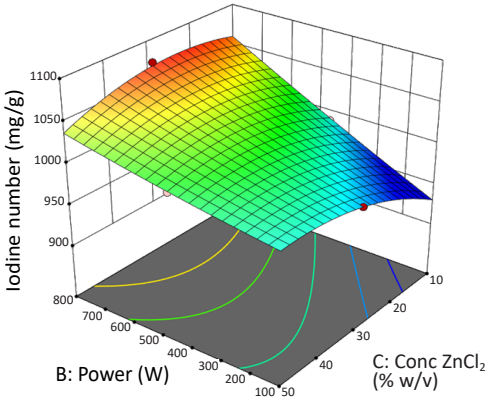

Figure 3. Three-dimensional response surface of iodine number for interaction between power microwave and $ZnCl_2$ concentration

the iodine number because the increase in heating time can damage the pore walls of the activated carbon (İzgi et al., 2019); the external shrinkage and carbon framework will collapse (Baytar, Şahin, & Saka, 2018). A prolonged heating time will decrease its absorption capability (Ao et al., 2018).

Figures 1 and 3 show the effect of microwave power on the iodine number. Figures 1 and 3 show that the result iodine number increases as microwave power increases. The study's findings showed that the iodine number increased from around 900 mg/g to approximately 1000 mg/g when the power was increased from 180 to 800 W. The increased iodine number value is due to activated carbon's ability to absorb microwave energy and modify pore structure. Furthermore, the formation of pore structure is enhanced by the interaction of $ZnCl_2$ and sample at high microwave energies (İzgi et al., 2019). The effect of microwave power on activating activated carbon is an increase in system temperature that promotes the formation of pores in the material (Junior et al., 2014). The system temperature and the sample temperature directly affect the microwave power. Activated carbon's removal of tar and volatile compounds is enhanced by increased temperatures (İzgi et al., 2019).

In addition, sample mass and microwave power are closely related. A higher microwave power level allows more energy to enter the pores, resulting in the development of the active side and larger pores in activated carbon (Ao et al., 2018). However, when microwave power reaches a limit, too much energy will cause the amount of carbon to burn and destroy the pore structure (Ao et al., 2018). It was proven in research conducted by (İzgi et al., 2019), where the value of the iodine number decreased at a microwave power of more than 800 W. According to other studies, the value of the iodine number decreases when the microwave power approaches 500 W (Baytar, Şahin, & Saka, 2018). Overheating activated carbon can diminish the number of mesopores and micropores in the material (Ayu, 2017).

The impact of $ZnCl_2$ concentration on the findings can be observed from Figures 2 and 3. The iodine number rises from 10 to 30% w/v in $ZnCl_2$ concentration. In comparison, activator concentrations beyond 30 to 50% w/v tend to decline the iodine number because low $ZnCl_2$ concentration cannot optimally activate raw material. In contrast, when the activator concentration is high, activated carbon develops a macroporous structure (Teğin et al., 2020). In addition, alterations in the pore structure of the activated carbon promote the decrease in iodine number. The interaction between the sample and excess

$ZnCl_2$ destroys activated carbon's micropores and forms more mesopores and macropores (Baytar, Şahin, & Saka, 2018). High concentrations of $ZnCl_2$ will promote pore collapse and destroy activated carbon's micropores (Özhan et al., 2014). Furthermore, an increase in the impregnation ratio that is too high has a negative effect, which causes combustion and clogs the pores due to an excessive amount of reagent, which reduces the access area of carbon (Ao et al., 2018).

The experimental design, as well as the responses and the predictions that were obtained, are presented in Table 3. In this study, responses were provided as iodine numbers. The iodine number is the defining characteristic of activated carbon. The iodine number is determined by the surface area of pores having a radius greater than 1 nm. Iodine adsorption was used to investigate the pore structure of activated carbon (Teğin et al., 2020). The statistical significance and components of the model were evaluated using ANOVA with a 95% confidence level. Table 4 presents the findings of the ANOVA analysis. Table 4 shows that model terms B, AB, BC, A^2, and C^2 are statistically significant. Based on Table 4, BBD terms are considered statistically significant when the *p*-value <0.05 under the selection condition, while the *p*-value >0.05 in the BBD model is disregarded (Jawad et al., 2020). The correlation of a second-order polynomial equation between input parameters and the response is given in Equation 2.

$$Y=1012.45+12.32B+30.91AB-21.40BC+8.14A^2-19.56C^2 \quad [2]$$

The BBD model can also be validated graphically by analyzing the residual distribution's characteristics and the correlation between the actual and predicted iodine number values (Jawad et al., 2020). The normal probability versus externally studentized residuals are shown in Figure 4a. This plot determines that the residuals are normally distributed. The points in a normal distribution should be in an approximately straight line. Since the points in Figure 4a are in a straight line, it can be inferred that they are normally distributed. The residuals' normal distributions represent both the residuals' independence and the validity of the assumptions (Reghioua et al., 2021). Figure 4b shows the correlation between the iodine number's actual and predicted values. According to Figure 4b, the predicted and actual points were mostly close. This finding indicates that the experimental results of this study are acceptable.

Therefore, the Model *F*-value of 34.49 implies that the model is significant. There is only a 0.06% chance that an F-value this large could occur due to noise. The Lack of Fit *F*-value of 0.69 implies that the Lack of Fit is not significant relative to the pure error. There is a 63.84% chance that a Lack of Fit *F*-value this large could occur due to noise. A non-significant lack of fit is good, meaning the model is significant. The model has the adjusted R^2 of 0.9556, and the predicted R^2 of 0.8537 are reasonably in agreement. The significant model requires a difference of less than 0.2. A high correlation coefficient (R^2 =

0.9556) indicated the high combability between expected and experimental values (Jawad et al., 2021).

Table 3
Experimental design of BBD with 3-variables and experimental data for iodine number

Run	Variable			Responses Y = iodine number (mg/g)	
	A	B	C	Actual	Predicted
1	7	450	30	1015.89	1012.45
2	12	100	30	981.87	981.79
3	12	800	30	1072.31	1068.24
4	2	800	30	1002.40	1002.48
5	7	100	50	1008.78	1007.74
6	2	450	10	1003.70	1002.58
7	2	450	50	998.56	995.53
8	2	100	30	1035.60	1039.66
9	7	450	30	1015.89	1012.45
10	12	450	10	989.82	992.85
11	7	100	10	961.27	958.32
12	7	800	50	986.65	989.59
13	7	450	30	1005.56	1012.45
14	12	450	50	1012.03	1013.15
15	7	800	10	1024.72	1025.75

Table 4
Analysis of variance (ANOVA) for the iodine number

Source	Sum of Squares	*df*	Mean Square	*F*-value	*p*-value
Model	8969.67	9	996.63	34.49	0.0006
A-Heating time	31.06	1	31.06	1.07	0.3473
B-Power	1214.09	1	1214.09	42.02	0.0013
C-Conc $ZnCl_2$	87.85	1	87.85	3.04	0.1417
AB	3821.40	1	3821.40	132.26	< 0.0001
AC	186.98	1	186.98	6.47	0.0517
BC	1831.11	1	1831.11	63.37	0.0005
A^2	244.38	1	244.38	8.46	0.0335
B^2	22.37	1	22.37	0.7744	0.4191
C^2	1411.94	1	1411.94	48.87	0.0009
Residual	144.47	5	28.89		
Lack of Fit	73.33	3	24.44	0.6872	0.6384
Pure Error	71.14	2	35.57		
Cor Total	9114.14	14			

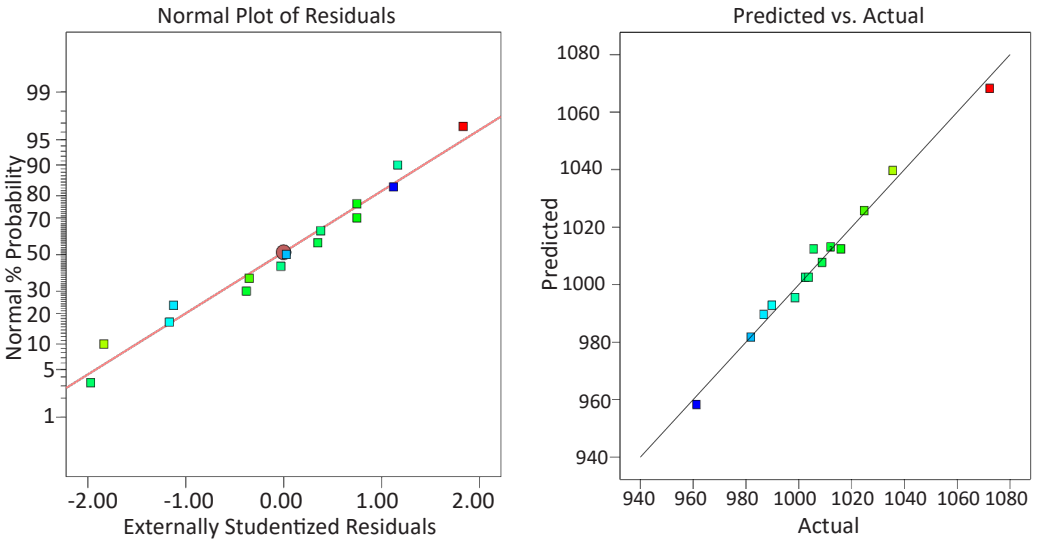

Figure 4. Normal probability plot of residuals for (a) BBD model (a), (b) plot of the relationship between the predicted and actual value of iodine number (mg/g)

Optimization Process

The optimum conditions for synthesizing activated carbon or process variables can be determined using the iodine number. Design Experts determined the optimal conditions for the synthesis of activated carbon. The process conditions were optimized if the desirability was close to 1. (Junior et al., 2014). A response with a desirable value of 1 indicates that it was received. In contrast, a desirability rating of 0 indicates that the response value exceeds the acceptable threshold (Jawad et al., 2021). The main objective is determining the point at which desirability is at its maximum level. A desirability function is thus a well-established method for determining the simultaneous optimization of process variables (A: $ZnCl_2$ concentration, B: Heating Time, C: Microwave Power) that produces the best performance level for the response (Iodine Number mg/g).

The numerical optimization showed the best iodine number was produced at 24.281% $ZnCl_2$, 12 minutes of heating time, and 800 W of microwave power; at these operating parameters, the iodine number is 1068.24 mg/g with a desirability value of 0.968 as shown in Figure 5. Overall, there was a good correlation between the results from numerical optimization utilizing desirability functions and the results from actual data. The actual iodine number is 1072.31 mg/g. The predicted and actual results have a relatively low error value of 2.035%, which means there is little difference between the actual and predicted values. The study shows that the BBD model with desirability functions may be successfully utilized to optimize the experimental condition for synthesizing activated carbon using microwave-assisted chemical activation (Jawad et al., 2021).

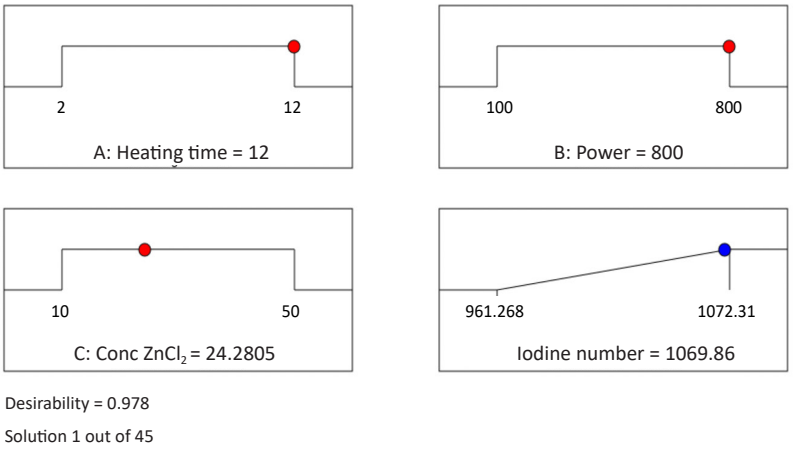

Figure 5. Desirability ramps for the optimization of preparation activated carbon input parameters for iodine number by Microwave-assisted $ZnCl_2$ chemical activation

Characterization of Activated Carbon

Moisture Content. The moisture content of activated carbon can affect the adsorption process. The lower the moisture content of activated carbon, the emptier pores can be filled by the adsorbate, allowing for an optimum adsorption process. The relatively low moisture content of activated carbon implies that water has evaporated during the carbonation and activation processes (Tasanif et al., 2020). In this study, the moisture content of activated carbon ranged from 5.51 to 9.21%. The study showed that the moisture content of activated carbon agreed with Indonesian National Standard (SNI) 06-3730-1995, which stated that the water content of powdered activated carbon should not exceed 15%.

FT-IR Analysis. Figure 6 shows the FTIR test results for bagasse, carbon, and activated carbon. FTIR tests on bagasse showed a band of hydroxyl groups (O-H) at wave numbers around 3400–3500 cm^{-1}, C-H bonds at 2800–2900 cm^{-1}, and a C=C bond at 1500–1600 cm^{-1}. It is similar to a study that reported most agricultural waste, including cellulose, hemicellulose, and lignin, had wave numbers between 3412 and 3392 cm^{-1}, indicating the presence of O-H groups (Vo et al., 2019). O-H functional groups (3590–3650 cm^{-1}), hydrogen bonds, and C-H bonds (2850–2970 cm^{-1}) derived from cellulose, as well as C=C bonds (1500–1600 cm^{-1}) derived from lignin aromatic rings, are also present in bagasse (Pratama et al., 2018) The results of the analysis of carbon and activated carbon are similar in Figure 6. The lack of peaks at wave numbers 3400–3500 cm^{-1} and 2800–2900 cm^{-1} in the results of the FTIR analysis of carbon and activated carbon indicates that the O–H bond and the C–H bond have degraded. A monomer group replaces the O-H group, formerly a hydrogen bond. The O-H groups will attach to aromatic compounds as a result of the

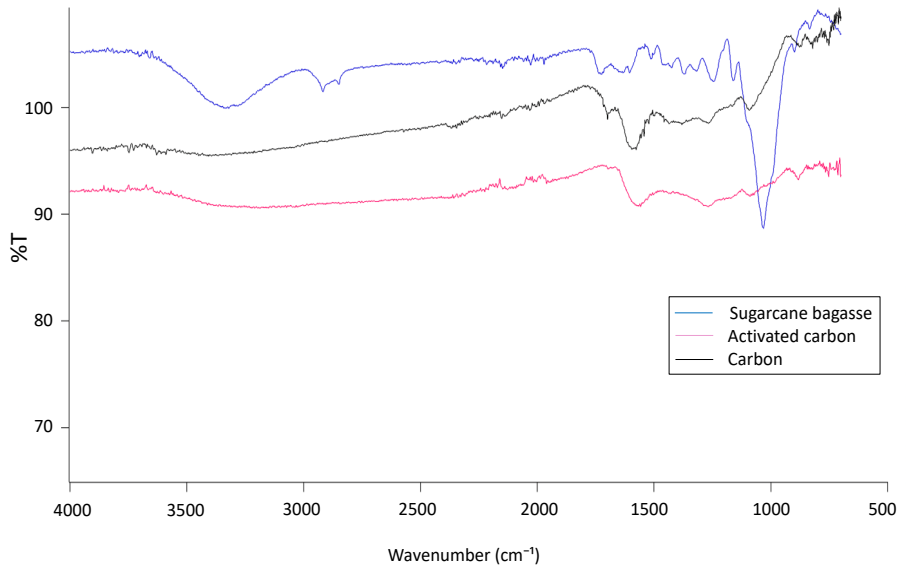

Figure 6. FT-IR analysis for sugarcane bagasse, carbon, and activated carbon

cellulose molecules' aromatization into polyaromatic structures during the carbonation and activation processes (Pratama et al., 2018). A C=O (carbonyl compound) bond is indicated at wave numbers between 1870 cm^{-1} and 1650 cm^{-1} in carbon and activated carbon. The presence of the C=O group, which denotes carbonyl acid stretching and is a characteristic group found in activated carbon, indicates that bagasse has generated a carbon-active material (Ayu, 2017). The difference between carbon and activated carbon can be seen in the wave numbers between 800 cm^{-1} and 1000 cm^{-1}, which indicate the presence of C-Cl bonds as a result of the $ZnCl_2$ activation process (Vo et al., 2019).

Morphological structure. SEM analysis has been performed on the surface morphology of activated carbon. Figure 7 shows the 1000x SEM results on sugarcane bagasse, carbon, and activated carbon. Figure 7(a) shows the scanning electron microscopy (SEM) results of untreated bagasse; the bagasse's surface is smooth and has slight cracks and voids. Figure 7(b) shows the scanning electron microscope (SEM) analysis of carbon bagasse, showing that a porosity structure with an irregular pore structure has formed. While Figure 7(c) shows the scanning electron microscopy (SEM) study results on activated carbon following the activation process, the pores generated are more numerous and not uniform besides the surface of the activated carbon developing cavities.

The heating method with a furnace and microwave promotes the formation of irregular pores and cavities on the surface of activated carbon (İzgi et al., 2019). Heating in furnaces and microwaves leads to the evaporation of carbon components like lignin and organic matter, forming pores in activated carbon [Figure 7(c)]. These pores can be mesoporous

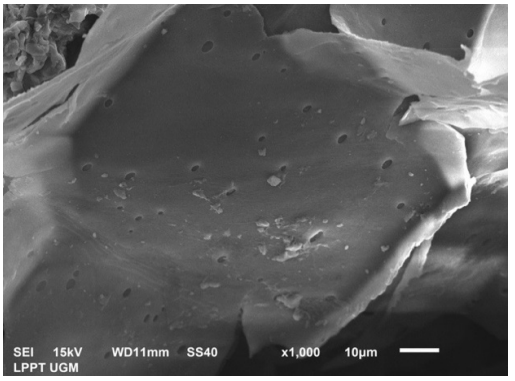

(a) sugar bagasse

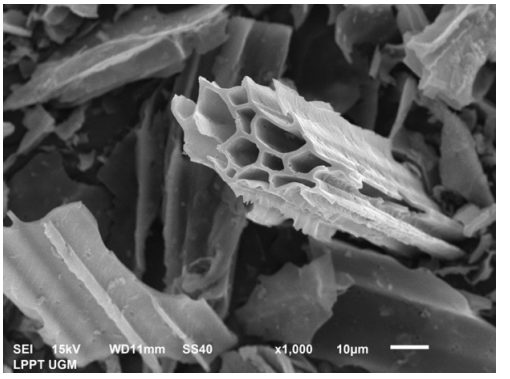

(b) carbon

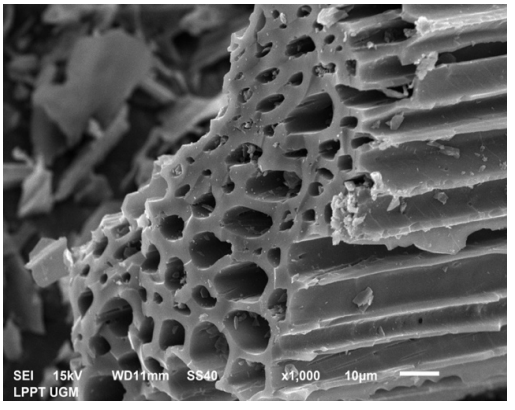

(c) activated carbon

Figure 7. Scanning electron microscope (SEM) analysis of (a) sugarcane bagasse, (b) carbon, and (c) activated carbon at optimum conditions

or microporous, depending on the size of the pores that are created (Labied et al., 2018). Activated carbon and carbon have a surface that seems rougher than raw material. The chemical and thermal activation of activated carbon generates mesopores and micropores, and then the pores of activated carbon cause the surface to be rougher (Labied et al., 2018). Furthermore, activating activated carbon employs a high-power microwave, causing a surface to become rougher (Tran et al., 2016).

Specific surface area and pore structure. The N_2 adsorption-desorption isotherm and pore size distribution are shown in Figure 8. Figure 8(a) shows the adsorption-desorption isotherm of an activated carbon with a type IV isotherm according to IUPAC standards. Isotherms type IV show that the pores generated are mesopores with small pore diameters (Horvat et al., 2022). Thommes et al. (2015) stated that type IV isotherms generate mesopore adsorbents with cylinder and conical geometries that are closed at the ends. The adsorption-desorption isotherm of activated carbon has a hysterical loop, as shown in Figure 8(a). Since the amount of N_2 gas adsorbed is not equal to that of adsorbed, hysteresis indicates that pore condensation occurred during adsorption (Luo et al., 2019). According to Thommes et al. (2015), loop hysteresis on BAC_{op} is classified as hysterical H4, which exhibits slit-shaped pore material and is frequently observed on micro-mesoporous carbon. Hysteresis Loop H4 indicates a complex interaction with micro and mesopore (Horvat et al., 2022).

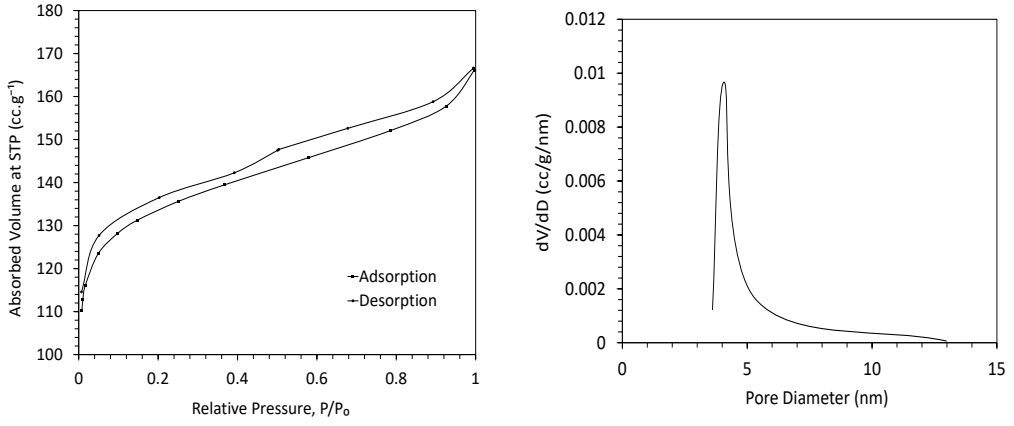

(a) (b)

Figure 8. (a) N_2 Adsorption-desorption isotherm of AC_{op} and (b) Barret-Joyner-Halenda BJH Corresponding Pore size distribution of AC_{op}

Figure 8 shows the Barret-Joyner-Halenda (BJH) pore size distribution of BAC_{op}. Most BAC_{op} pores have a diameter between 3.5 and 5.4 nm, indicating that BAC_{op} pores are part of the mesopore. The pore volume of BAC_{op} is 0.054 cc/g, the average pore diameter is 4.071 nm, and the total pore volume is 0.2531 cc/g. It has a surface area of 446.874 m^2/g. Table 5 compares the surface area of activated carbon with several previous studies. Based on the BET study, the average pore width of BAC_{op} is 4.071 nm, with pore sizes ranging from 3.5 to 5.4 nm. Based on the average pore width and the pore size distribution, BAC_{op} may adsorb chromium ions with a molecular size of less than 0.088 nm (Labied et al., 2018).

CONCLUSION

This study reported the synthesis of activated carbon from bagasse by $ZnCl_2$ using microwave-assisted activation. Optimizing the condition of the AC synthesis process has been accomplished with effectiveness utilizing the response surface methodology approach. The BAC optimization (BAC_{op}) was at a $ZnCl_2$ concentration of 24.281 (%w/v), 12 minutes of heating time, and 800 W of microwave power. The characterization results show that BAC_{op} has mesoporous carbon and a desirable surface area of 446.874 m^2/g, average pore size of 4.071 nm, pore volume of 0.054 cc/g, and total pore volume of 0.2531 cc/g. SEM analysis revealed that microwave-generated pore structures lead to the $ZnCl_2$ activation process. The FT-IR analysis shows the existence of functional groups as well as changes in functional groups from raw material to activated carbon. The moisture content study findings are 5.51 to 9.21% in accordance with the Indonesian National Standard (SNI) 06-3730-1995. The isothermal adsorption-desorption process is classified as type IV adsorption with hysteresis loop H4, suggesting that the pore distribution in activated carbon is mesoporous with a tiny pore width and slit-shape pore materials.

ACKNOWLEDGEMENTS

We thank Badan Pemberdayaan Sumber Daya Manusia Industri Industry Ministry, Indonesia for financial support. We are also thankful to the Laboratory of Chemistry, Department of Leather Processing Technology, Politeknik ATK Yogyakarta, Indonesia for providing the facilities for our study.

REFERENCES

Abdulhameed, A. S., Firdaus Hum, N. N. M., Rangabhashiyam, S., Jawad, A. H., Wilson, L. D., Yaseen, Z. M., Al-Kahtani, A. A., & Alothman, Z. A. (2021). Statistical modeling and mechanistic pathway for methylene blue dye removal by high surface area and mesoporous grass-based activated carbon using K_2CO_3 activator. *Journal of Environmental Chemical Engineering*, *9*(4), Article 105530. https://doi.org/10.1016/j.jece.2021.105530

Ao, W., Fu, J., Mao, X., Kang, Q., Ran, C., Liu, Y., Zhang, H., Gao, Z., Li, J., Liu, G., & Dai, J. (2018). Microwave assisted preparation of activated carbon from biomass: A review. *Renewable and Sustainable Energy Reviews*, *92*, 958-979. https://doi.org/10.1016/j.rser.2018.04.051

Arnelli, A., Putri, U. H. H., Cholis, F. N., & Astuti, Y. (2019). Use of microwave radiation for activating carbon from rice husk using $ZnCl_2$ activator. *Jurnal Kimia Sains dan Aplikasi*, *22*(6), 283-291. https://doi.org/10.14710/jksa.22.6.283-291

Ayu, G. E. (2017). *Pembuatan karbon aktif dari tempurung kelapa (coconut shell) dengan proses pengaktifan kimia $ZnCl_2$ menggunakan microwave* [Preparation of activated carbon from coconut shell using Microwave-assisted $ZnCl_2$ Chemical activation]. [Doctoral dissertation]. Universitas Sumatera Utara, Indonesia. http://repositori.usu.ac.id/handle/123456789/20774

Baytar, O., Şahin, Ö., & Saka, C. (2018). Sequential application of microwave and conventional heating methods for preparation of activated carbon from biomass and its methylene blue adsorption. *Applied Thermal Engineering*, *138*, 542-551. https://doi.org/10.1016/j.applthermaleng.2018.04.039

Baytar, O., Şahin, Ö., Saka, C., & Ağrak, S. (2018). Characterization of microwave and conventional heating on the pyrolysis of pistachio shells for the adsorption of methylene blue and iodine. *Analytical Letters*, *51*(14), 2205-2220. https://doi.org/10.1080/00032719.2017.1415920

Bian, Y., Yuan, Q., Zhu, G., Ren, B., Hursthouse, A., & Zhang, P. (2018). Recycling of waste sludge: Preparation and application of sludge-based activated carbon. *International Journal of Polymer Science*, Article 8320609. https://doi.org/10.1155/2018/8320609

Buthiyappan, A., Gopalan, J., & Raman, A. A. A. (2019). Synthesis of iron oxides impregnated green adsorbent from sugarcane bagasse: Characterization and evaluation of adsorption efficiency. *Journal of Environmental Management*, *249*, Article 109323. https://doi.org/10.1016/j.jenvman.2019.109323

Daochalermwong, A., Chanka, N., Songsrirote, K., Dittanet, P., Niamnuy, C., & Seubsai, A. (2020). Removal of heavy metal ions using modified celluloses prepared from pineapple leaf fiber. *ACS Omega*, *5*(10), 5285-5296. https://doi.org/10.1021/acsomega.9b04326

Deng, H., Yang, L., Tao, G., & Dai, J. (2009). Preparation and characterization of activated carbon from cotton stalk by microwave assisted chemical activation-application in methylene blue adsorption from aqueous solution. *Journal of Hazardous Materials*, *166*(2-3), 1514-1521. https://doi.org/10.1016/j.jhazmat.2008.12.080

Elsayed, M. A., & Zalat, O. A. (2015). Factor affecting microwave assisted preparation of activated carbon from local raw materials. *International Letters of Chemistry, Physics and Astronomy*, *47*, 15-23. https://doi.org/10.18052/www.scipress.com/ilcpa.47.15

el Nemr, A., Aboughaly, R. M., el Sikaily, A., Masoud, M. S., Ramadan, M. S., & Ragab, S. (2022). Microporous-activated carbons of type I adsorption isotherm derived from sugarcane bagasse impregnated with zinc chloride. *Carbon Letters*, *32*(1), 229-249. https://doi.org/10.1007/s42823-021-00270-1

Foo, K. Y., Lee, L. K., & Hameed, B. H. (2013). Preparation of activated carbon from sugarcane bagasse by microwave assisted activation for the remediation of semi-aerobic landfill leachate. *Bioresource Technology*, *134*, 166-172. https://doi.org/10.1016/j.biortech.2013.01.139

Hidayati, A. S. D. S. N., Kurniawan, S., Restu, N. W., & Ismuyanto, B. (2016). Potensi ampas tebu sebagai alternatif bahan baku pembuatan karbon aktif [Potential sugarcane bagasse as an alternative raw material for activated carbon production]. *Natural B*, *3*(4), 311-317.

Horvat, G., Pantić, M., Knez, Ž., & Novak, Z. (2022). A brief evaluation of pore structure determination for bioaerogels. *Gels*, *8*(7), Article 438. https://doi.org/10.3390/gels8070438

İzgi, M. S., Saka, C., Baytar, O., Saraçoğlu, G., & Şahin, Ö. (2019). Preparation and characterization of activated carbon from microwave and conventional heated almond shells using phosphoric acid activation. *Analytical Letters*, *52*(5), 772-789. https://doi.org/10.1080/00032719.2018.1495223

Jawad, A. H., Abdulhameed, A. S., Hanafiah, M. A. K. M., ALOthman, Z. A., Khan, M. R., & Surip, S. N. (2021). Numerical desirability function for adsorption of methylene blue dye by sulfonated pomegranate peel biochar: Modeling, kinetic, isotherm, thermodynamic, and mechanism study. *Korean Journal of Chemical Engineering*, *38*(7), 1499-1509. https://doi.org/10.1007/s11814-021-0801-9

Jawad, A. H., Mohammed, I. A., & Abdulhameed, A. S. (2020). Tuning of fly ash loading into chitosan-ethylene glycol diglycidyl ether composite for enhanced removal of reactive red 120 dye: Optimization using the box–behnken design. *Journal of Polymers and the Environment*, *28*(10), 2720-2733. https://doi.org/10.1007/s10924-020-01804-w

Jiang, W., Zhang, L., Guo, X., Yang, M., Lu, Y., Wang, Y., Zheng, Y., & Wei, G. (2021). Adsorption of cationic dye from water using an iron oxide/activated carbon magnetic composites prepared from sugarcane bagasse by microwave method. *Environmental Technology*, *42*(3), 337-350. https://doi.org/10.1080/09593330.2019.1627425

Junior, O. P., Cazetta, A. L., Gomes, R. C., Barizão, É. O., Souza, I. P. A. F., Martins, A. C., Asefa, T., & Almeida, V. C. (2014). Synthesis of $ZnCl_2$-activated carbon from macadamia nut endocarp (*Macadamia integrifolia*) by microwave-assisted pyrolysis: Optimization using RSM and methylene blue adsorption. *Journal of Analytical and Applied Pyrolysis*, *105*, 166-176. https://doi.org/10.1016/j.jaap.2013.10.015

Karri, R. R., Sahu, J. N., & Meikap, B. C. (2020). Improving efficacy of Cr (VI) adsorption process on sustainable adsorbent derived from waste biomass (sugarcane bagasse) with help of ant colony optimization. *Industrial Crops and Products, 143*, Article 111927. https://doi.org/10.1016/j.indcrop.2019.111927

Kaushik, A., Basu, S., Singh, K., Batra, V. S., & Balakrishnan, M. (2017). Activated carbon from sugarcane bagasse ash for melanoidins recovery. *Journal of Environmental Management*, *200*, 29-34. https://doi.org/10.1016/j.jenvman.2017.05.060

Labied, R., Benturki, O., Hamitouche, A. Y. E., & Donnot, A. (2018). Adsorption of hexavalent chromium by activated carbon obtained from a waste lignocellulosic material (*Ziziphus jujuba* cores): Kinetic, equilibrium, and thermodynamic study. *Adsorption Science and Technology*, *36*(3-4), 1066-1099. https://doi.org/10.1177/0263617417750739

Lam, S. S., Liew, R. K., Wong, Y. M., Yek, P. N. Y., Ma, N. L., Lee, C. L., & Chase, H. A. (2017). Microwave-assisted pyrolysis with chemical activation, an innovative method to convert orange peel into activated carbon with improved properties as dye adsorbent. *Journal of Cleaner Production*, *162*, 1376-1387. https://doi.org/10.1016/j.jclepro.2017.06.131

Luo, X., Cai, Y., Liu, L., & Zeng, J. (2019). Cr(VI) adsorption performance and mechanism of an effective activated carbon prepared from bagasse with a one-step pyrolysis and $ZnCl_2$ activation method. *Cellulose*, *26*(8), 4921-4934. https://doi.org/10.1007/s10570-019-02418-9

Mahmood, T., Ali, R., Naeem, A., Hamayun, M., & Aslam, M. (2017). Potential of used *Camellia sinensis* leaves as precursor for activated carbon preparation by chemical activation with H_3PO_4; optimization using response surface methodology. *Process Safety and Environmental Protection*, *109*, 548-563. https://doi.org/10.1016/j.psep.2017.04.024

Ozdemir, I., Şahin, M., Orhan, R., & Erdem, M. (2014). Preparation and characterization of activated carbon from grape stalk by zinc chloride activation. *Fuel Processing Technology*, *125*, 200-206. https://doi.org/10.1016/j.fuproc.2014.04.002

Özhan, A., Şahin, Ö., Küçük, M. M., & Saka, C. (2014). Preparation and characterization of activated carbon from pine cone by microwave-induced $ZnCl_2$ activation and its effects on the adsorption of methylene blue. *Cellulose*, *21*(4), 2457-2467. https://doi.org/10.1007/s10570-014-0299-y

Pratama, B. S., Aldriana, P., Bambang, Ismuyanto., & Saptati, A. S. D. (2018). Konversi ampas tebu menjadi biochar dan karbon aktif untuk penyisihan Cr (VI) [Conversion of sugarcane bagasse to biochar and activated carbon for Cr(VI) removal]. *Jurnal Rekayasa Bahan Alam Dan Energi Berkelanjutan*, *2*(1), 7-12. http://rbaet.ub.ac.id/index.php/rbaet/article/view/45

Puchana-Rosero, M. J., Adebayo, M. A., Lima, E. C., Machado, F. M., Thue, P. S., Vaghetti, J. C. P., Umpierres, C. S., & Gutterres, M. (2016). Microwave-assisted activated carbon obtained from the sludge of tannery-treatment effluent plant for removal of leather dyes. *Colloids and Surfaces A: Physicochemical and Engineering Aspects*, *504*, 105-115. https://doi.org/10.1016/j.colsurfa.2016.05.059

Reghioua, A., Barkat, D., Jawad, A. H., Abdulhameed, A. S., Al-Kahtani, A. A., & Alothman, Z. A. (2021). Parametric optimization by Box-Behnken design for synthesis of magnetic chitosan-benzil/ZnO/Fe_3O_4 nanocomposite and textile dye removal. *Journal of Environmental Chemical Engineering*, *9*(3), Article 105166. https://doi.org/10.1016/j.jece.2021.105166

Salihi, I. U., Kutty, S. R. M., & Isa, M. H. (2017). Adsorption of lead ions onto activated carbon derived from sugarcane bagasse. *IOP Conference Series: Materials Science and Engineering*, *201*(1), Article 012034. https://doi.org/10.1088/1757-899X/201/1/012034

Sinyoung, S., Chaiwat, W., & Kunchariyakun, K. (2021). Preparation of activated carbon from bagasse by microwave-assisted phosphoric acid activation. *Walailak Journal of Science and Technology*, *18*(16), Article 22796. https://doi.org/10.48048/wjst.2021.22796

Siragi D. B. M., Desmecht, D., Hima, H. I., Mamane, O. S., & Natatou, I. (2021). Optimization of activated carbons prepared from *Parinari macrophylla* shells. *Materials Sciences and Applications*, *12*(05), 207-222. https://doi.org/10.4236/msa.2021.125014

Suhdi, & Wang, S. C. (2021). Fine activated carbon from rubber fruit shell prepared by using $ZnCl_2$ and KOH activation. *Applied Sciences*, *11*(9), Article 3994. https://doi.org/10.3390/app11093994

Tasanif, R., Isa, I., & Kunusa, W. R. (2020). Potensi ampas tebu sebagai adsorben logam berat Cd, Cu dan Cr [Potential of sugarcane bagasse as an adsorbent for heavy metals Cd, Cu and Cr]. *Journal of Chemistry*, *2*(1), 34-44.

Teğin, Ş. Ö., Şahin, Ö., Baytar, O., & İzgi, M. S. (2020). Preparation and characterization of activated carbon from almond shell by microwave-assisted using $ZnCl_2$ activator. *International Journal of Chemistry and Technology*, *4*(2), 130-137. https://doi.org/10.32571/ijct.747943

Thommes, M., Kaneko, K., Neimark, A. V., Olivier, J. P., Rodriguez-Reinoso, F., Rouquerol, J., & Sing, K. S. W. (2015). Physisorption of gases, with special reference to the evaluation of surface area and pore size distribution (IUPAC Technical Report). *Pure and Applied Chemistry*, *87*(9-10), 1051-1069. https://doi.org/10.1515/pac-2014-1117

Tran, T. V., Pham, V. T., Quynh, N. T. P., Cong, H. T., Tam, D. T. T., Thuan, V. N., & Bach, L. G. (2016). Production of activated carbon from sugarcane bagasse by chemical activation with $ZnCl_2$: Preparation and characterization study. *Research Journal of Chemical Sciences*, *6*(5), 42-47.

Ummartyotin, S., & Pechyen, C. (2016). Strategies for development and implementation of bio-based materials as effective renewable resources of energy: A comprehensive review on adsorbent technology. *Renewable and Sustainable Energy Reviews*, *62*, 654-664. https://doi.org/10.1016/j.rser.2016.04.066

Vo, A. T., Nguyen, V. P., Ouakouak, A., Nieva, A., Doma, B. T., Tran, H. N., & Chao, H. P. (2019). Efficient removal of Cr(VI) from water by biochar and activated carbon prepared through hydrothermal carbonization and pyrolysis: Adsorption-coupled reduction mechanism. *Water*, *11*(6), Article 1164. https://doi.org/10.3390/w11061164

Yuan, Z., Xu, Z., Zhang, D., Chen, W., Zhang, T., Huang, Y., Gu, L., Deng, H., & Tian, D. (2018). Box-Behnken design approach towards optimization of activated carbon synthesized by co-pyrolysis of waste polyester textiles and $MgCl_2$. *Applied Surface Science*, *427*, 340-348. https://doi.org/10.1016/j.apsusc.2017.08.241